Invited Paper

Strongly coupled multicore fiber with FBGs for multipoint and multiparameter sensing

Zhiming Liu[1], Di Zheng[1*], Javier Madrigal[2], Joel Villatoro[3,4], Enrique Antonio-Lopez[5], Axel Schülzgen[5], Rodrigo Amezcua-Correa[5], Xihua Zou[1], Wei Pan[1] and Salvador Sales[2]

[1]Center for Information Photonics & Communications, School of Information Science & Technology, Southwest Jiaotong University, Chengdu, 610031, China
[2]Photonics Research Labs, ITEAM Research Institute, Universitat Politècnica de València, Camino de Vera, s/n, 46022, Valencia, Spain
[3]Department of Communications Engineering, University of the Basque Country UPV/EHU, Plaza Torres Quevedo 1, E-48013, Bilbao, Spain
[4]IKERBASQUE - Basque Foundation for Science, Bilbao, E-48011, Spain.
[5]University of Central Florida, CREOL the College of Optics and Photonics, Orlando, 162700, Florida, USA.
*Corresponding author: dzheng@home.swjtu.edu.cn

ABSTRACT

A compact optical fiber sensor by embedding fiber Bragg gratings (FBGs) in strongly coupled multicore fiber (SCMCF) is proposed for multipoint and multiparameter sensing. To build the device, two FBGs with different peak wavelengths were inscribed in a segment of SCMCF. Then one end of the SCMCF was fusion spliced to a single-mode fiber (SMF) and the other end of the SCMCF was cleaved. In the SMF-SCMCF structure, two supermodes are excited, as a result, the reflection spectrum exhibits a sinusoidal pattern with two sharp peaks. The wavelength position of the FBGs and the supermode coupler can be extracted simultaneously. Two distinct FBGs inscribed in different positions of the SCMCF were used to demonstrate quasi-distributed multipoint sensing in the proposed structure. To the best of our knowledge, this is the first demonstration of an optical fiber sensor that combines FBGs with SCMCF. The sensor here proposed has the advantage of compact size, low-cost, good mechanical strength and ease of interrogation.

Keywords: Optical fiber sensor, Multicore optical fiber, Fiber Bragg gratings

I. INTRODUCTION

Over the past decades, optical fiber sensors have been widely used in the fields of civil engineering, mechanical manufacturing, robotics and aeronautical engineering due to its unique characteristics such as immunity to electromagnetic interference, resistant to corrosion, high sensitivity and compact size [1,2]. So far, various optical fiber sensors have been developed based on different sensing principles, such as long period gratings, fiber Bragg gratings (FBGs), Fabry-Perot interferometers, Mach–Zehnder interferometers, and so on [3-6]. Among them, FBG-based

sensors are one of the most representative and promising optical fiber sensing technique due to their mature manufacturing process and multiplexing capability.

A variety of FBG-based sensors have been validated in different types of optical fibers, such as single-mode fiber (SMF), multimode fiber, photonic crystal fiber, microstructure fiber, polymer fiber and multicore fiber (MCF) [7-13], just to mention a few. Compared with other types of optical fiber, MCF comprises more than one core within the same cladding. Consequently, several identical or different sensors can be written at the same position along the length of the MCF, which is beneficial for simultaneous measurement of multiple parameters [14-16]. Therefore, multicore fiber Bragg grating (MCFBG) sensors have been proposed and successfully validated in a variety of mechanical parameters sensing, such as bending, twist, inclination, acceleration, or 3D shape sensing [17-22]. For instance, Gander et al. reported the first demonstration of bend sensing using a pair of FBGs written in a two-core MCF [23]. Soon afterwards, a two-axis bend measurement was realized by writing FBGs into three separate cores of a multicore fiber [24]. Apart from single-point measurement, Barrera et al. proposed a multipoint two-dimensional curvature sensor by inscribing arrays of apodized highly reflective FBGs in non-twisted homogeneous four-core MCF [25]. Fender et al. reported a two-axis temperature-insensitive accelerometer by inscribing pairs of FBGs into MCF to measure differential strain [21]. Distributed temperature and 3D shape sensing with high accuracy have been demonstrated by using continuous multicore fiber grating arrays [26]. It is noteworthy that the MCFBG-based sensors exhibit excellent ability to compensate the variation of environmental temperature. This is because all cores are embedded in the same cladding and, consequently, have same temperature response. So far, the majority of MCFBG-based sensors were fabricated by using weakly coupled MCF, where the coupling between neighboring cores can be negligible. In this case, the use of expensive fan-in/out devices to extract sensing information from individual cores is inevitable. Thus, weakly coupled MCFBG sensors tend to complex and more costly.

Recently, a new type of MCF known as strongly coupled muti-core fiber (SCMCF) has attracted research attention. In an SCMCF, the separation between the cores is small enough; hence, the evanescent fields of the guiding cores coupled to each other. Therefore, all cores of the SCMCF participate in the sensing task. An important advantage of SCMCFs is their simple interrogation as it can be carried out with a conventional SMF. This drastically simplifies the interrogation of SCMCF-based sensors. So far, several compact sensors based on SCMCFs have been reported for high-temperature, vibration or strain measurement [27-29]. However, such sensors are not suitable for multiparameter sensing. To solve this issue, FBGs were inscribed in SCMCF, in this manner two sensing structures can be obtained that can sensor two or more parameters has been demonstrated by other authors [30-32].

In this paper, we propose and demonstrate a novel optical fiber sensor for temperature, transverse load and vibration sensing. The proposed sensor is fabricated by inscribing two cascaded FBGs in an SCMCF, which is then spliced to SMF to form a SMF-SCMCF structure. In the latter configuration, two supermodes supported by the SCMCF give rise to a well-defined sinusodial pattern. The SMF-SCMCF structure was used as a vibration gauge, while two cascaded FBGs were dedicated to measure transverse load and temperature at different locations. The experimental results demonstrate that two consecutive FBGs can accurately measure the temperature and transverse load at two adjacent positions, while the periodic shift of reflection spectrum can be used

to monitor vibration with high precision.

II. OPERATION PRICIPLE AND DEVICE FABRICATION

The SCMCF used to design our sensor was fabricated at the facilities of the University of Central Florida (Orlando, USA). The SCMCF consists of seven identical cores made of germanium doped silica; one core located in the center of the fiber and other cores are arranged in a hexagonal pattern. A micrograph of the cross section of the SCMCF is shown in Fig. 1(a). All cores have the same size of 9.2 μm with small core-to-core pitch of 11μm, and the external diameter of the SCMCF is 140 μm. The numerical aperture (NA) of each core is 0.14, which is the similar as that of telecommunications SMF. The schematic structure of the proposed sensor is shown in Fig. 1(b). The fabrication of the structure is simple. First, FBGs with different Bragg wavelengths are written in the SCMCF. Then, one end of the SCMCF is fusion spliced to an SMF and the other end of the SCMCF is cleaved. The reflection spectrum of the structure shown in Fig.1 (b) consists of a periodic maxima and minima caused by supermode interference in the SCMCF and two distinct peaks generated from two FBGs.

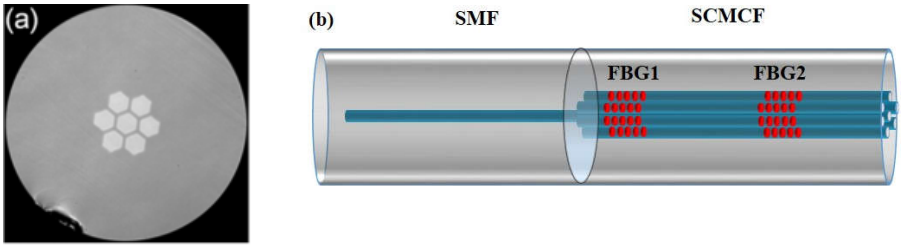

Fig. 1. (a) Micrograph of the cross section of the SCMCF. (b) Schematic structure of the proposed sensor.

The operating principle of the structure shown in Fig.1 (b) can be explained with coupled mode theory [33]. Note that the SMF-SCMCF structure is axially symmetric. The unique core of the SMF and the central core of the SCMCF are aligned. Under these conditions, only two supermodes that have intensity in the central core can be excited in the SCMCF by the fundamental mode of the SMF. The two supermodes have different effective refractive indices that can be termed as n_1 and n_2. According to [33], the reflection intensity of the light that is collected by the core of the SMF after being reflected from the cleaved end of the SCMCF can be expressed as:

$$I_R = 1 - (6/7)\sin^2(2\sqrt{7}\pi\Delta n L_f/\lambda) \quad (1)$$

In Eq. (1), $\Delta n = n_1 - n_2$, L_f is the length of the SCMCF segment and λ is the wavelength of the optical source. It is clearly that the supermodes in the SMF-SCMCF structure generates a periodic spectrum whose period dependents to the length of the SCMCF. When the SMF-SCMCF structure is exposed to vibrations, the bending-induced stress and strain will induce cyclic index changes to the supermodes, hence, cyclic changes of the position of the maximum in Eq. (1). As a consequence, vibrations can be detected as periodic shifts of the reflected pattern.

The experiment setup that we used to inscribe FBGs into the SCMCF is illustrated in Fig. 2. It is based on the phase-mask technique with the capability to write FBGs with various parameters. A frequency-doubled Argon-ion laser operating at 244 nm was used to inscribe FBGs in all cores of the SCMCF. The setup can be divided mainly into two subsystems: the laser beam conditioning subsystem and the optical fiber positioning subsystem. The laser beam conditioning subsystem is

exploited to inscribe precisely the FBGs in the SCMCF. It consists of a mirror mounted in a piezo-electric transducer that is used to induce a vertical deflection in the laser beam and two cylindrical lenses that tune the height and the width of the laser beam. The lenses and the phase mask are placed on a high precision linear stage controlled by a computer. The optical fiber positioning subsystem is composed of a pair of rotation stages that are placed on top of two three-axis translation stages and a vision system. Two rotation stages and two three-axis translation stages allow adjusting the distance between the optical fiber and the phase mask as well as the optical fiber inclination with high precision. A vision system is adopted to monitor the distance between the SCMCF and phase mask. The spatial location for the grating inscription is accurately adjusted using the high precision linear stage. Prior to the FBG inscription, the SCMCF was hydrogen-loaded at ambient temperature for two weeks at a pressure of 50 bar to increase its photosensitivity. Then, a section of the SCMCF with a length of 5 cm was immersed in analytical-grade acetone to facilitate the polymer coating removing. Finally, two 10 mm-long FBGs with ~30% reflectivity at 1543 and 1573 nm were written into all the cores of the SCMCF respectively, the separation between two FBGs is 2cm.

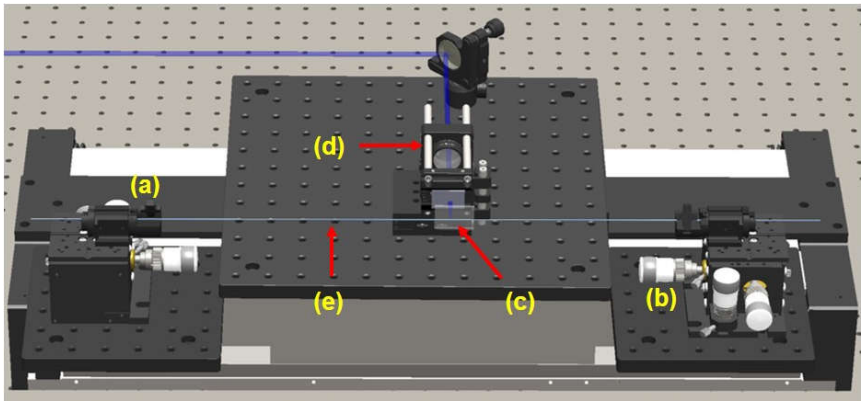

Fig.2. Experimental setup for inscribing FBGs in SCMCF with the phase-mask technique. (a) Rotation stages. (b) Translation stage. (c) Phase Mask. (d) Two cylindrical lenses. (e) SCMCF

As the NA of the SMF and the SCMCF are similar the insertion losses of our device can be minimal. The only important thing is to have high quality fusion splice between the SMF and the SCMCF. Thus, a high precision cleaver (Fujikura CT32) was used to cleave the SMF and the SCMCF. After cleaving, the fibers were cleaned with ethanol. Then, the junction between the SMF and the SCMCF was produced by using a fusion splicer (Fujikura FSM-45PM). The machine was configured to use the multimode mode fiber splicing program with a fusion arc time of 2000 ms. During the splicing process, the splicer used a cladding alignment method for which the unique core of the SMF and the central core of the SCMCF get precisely aligned, and subsequently the SMF and SCMCF were permanently joined together. It should be pointed out that, due to the SCMCF and SMF used here have the same NA of 0.14, the coupling between them can be maximized, which in turn benefits to lower the insertion loss. Besides, the SMF-SCMCF junction has been demonstrated to have high tensile strength, withstand up to thousands of microstrains, which ensures that the proposed sensor has enough mechanical strength for actual sensing applications [29].

III. RESULTS AND DISCUSSION

To measure the reflection spectrum of the device depicted in Fig.1(b), the output from a broadband light source is coupled into the proposed sensor through the lead-in SMF, then the

reflected signal pass through an optical circulator and consequently is measured by an optical spectrum analyzer (YOKOGAWA AQ6370D) with a resolution of 0.02 nm. Figure 3 shows the measured reflection spectrum of the proposed sensor. Note that the interference spectrum has well defined sinusoidal pattern and the minima close to 0. There are two distinctive peaks superimposed on the sinusoidal spectrum, which corresponds to two FBGs with the peak wavelength of 1543 and 1573 nm, respectively. It should be pointed out that although the circular cladding will lead to uneven illumination across the cores, all cores in SCMCF obtain almost uniform exposure due to the small core-pitch. Therefore, the peak wavelength discrepancy of FBGs from different cores is small, the overlapped reflection spectrum still features narrow peak, which is benefit to high-accuracy measurement.

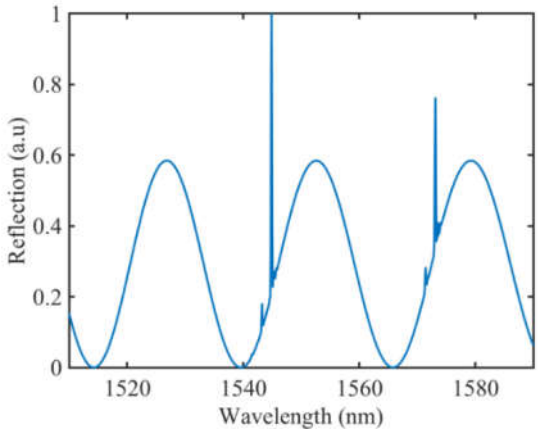

Fig.3. The measured reflection spectrum of the proposed sensor.

The feasibility of our device to multipoint temperature measurement was investigated first; the experimental setup used is shown in Fig.4. A ceramic thermometer with hollow tube structure was used to heat FBGs. The sensor goes through the ceramic tube and contacts with the inner wall of the ceramic tube. Due to the length of the ceramic tube is 1.2cm and the separation between two FBGs is 2 cm, which allow us to heat each FBG separately. The temperature was changed from 24 °C to 90 °C in steps of 10 °C, and each step was maintained for 10 minutes to guarantee that the FBG was subjected to a stable temperature environment.

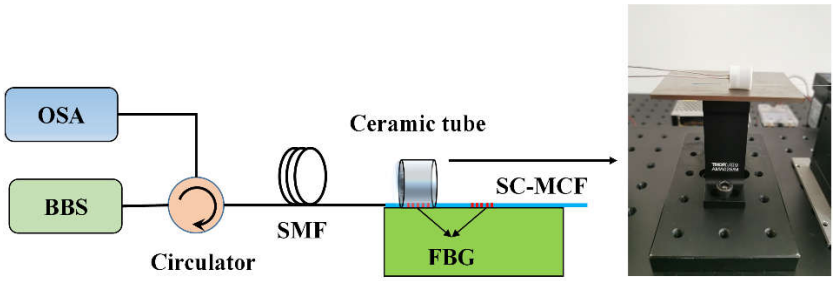

Fig.4. Schematic of the experiment setup for temperature sensing.

Figure 5 shows the response of the two FBGs to temperature. It can be clearly observed that the peak wavelength of both FBG exhibit a linear response to temperature and shift to longer wavelength with increasing temperature. The R^2 values of the linear fitting are all above 0.997. The temperature sensitivity of FBG1 and FBG2 are 9.77 pm/°C and 9.72 pm/°C, respectively. The wavelength resolution of the used OSA is 20 pm, thus, a temperature resolution of about 2°C can

be achieved with such an OSA. However, with an FBG interrogating system, which typically has picometer resolution, smaller temperature changes can be resolved.

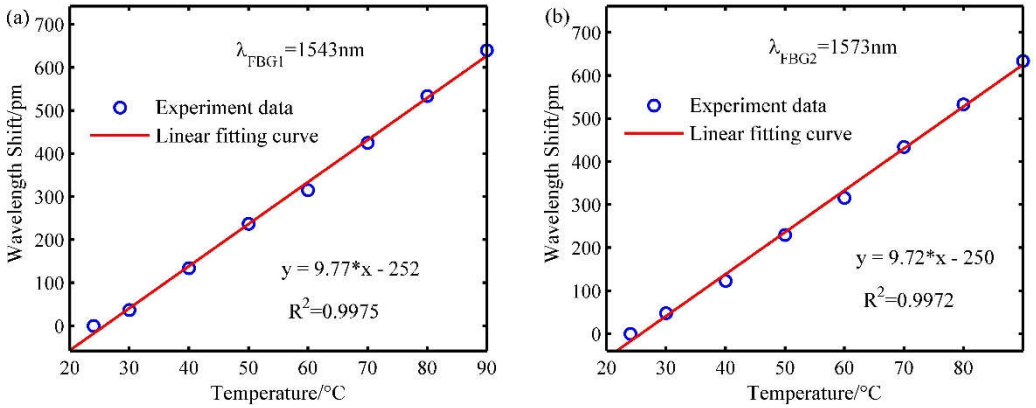

Fig.5. The wavelength shift of the two FBGs versus temperature. (a) FBG1; (b) FBG2

In order to investigate the sensor's repeatability and reliability, the temperature experiment was repeated three times. The measured discrepancy in wavelength shift at different temperature are shown in Fig. 6, the standard deviation based on triplet measurements are also included. The maximum discrepancy is less than 22 pm, which corresponds to a temperature uncertainty of 2.2°C. In fact, a ceramic thermometer used here has a temperature stability of ± 2 °C, which affected the measurement accuracy. With this in mind, the measurement accuracy of the temperature sensing can be further improved by using a more accurate temperature-controller device.

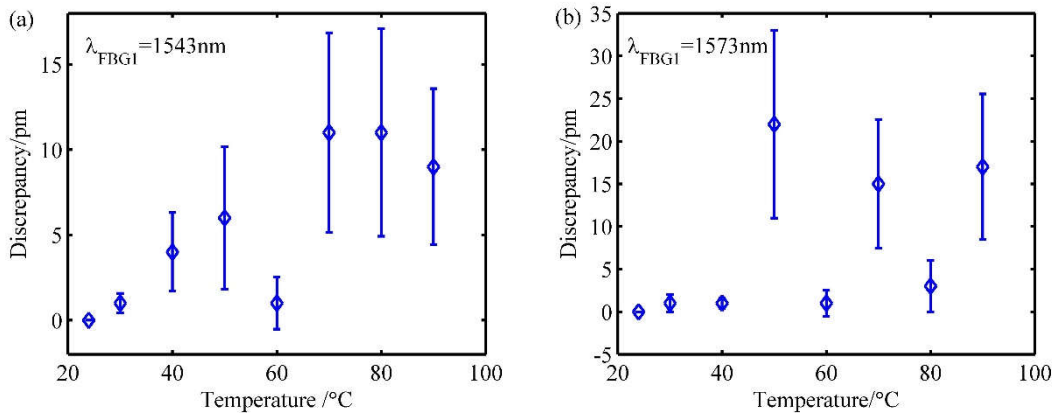

Fig.6. The discrepancy in wavelength shift of the two FBGs versus temperature. (a) FBG1; (b) FBG2

Multipoint transverse load sensing was investigated with the experimental setup shown in Fig. 7. A metal piece (width × length × thickness = 15 × 70 × 8 mm) with a mass of 0.07 kg was placed on the position of FBG located and a supporting fiber that used to balance the transverse load. The width of the metal piece is moderately larger than the length of FBG (10 mm), which ensures that one FBG is subjected to uniform lateral pressure while minimizes the impact on another adjacent FBG. During the experiment, the temperature was stabilized at ~25 °C. The transverse load response of two FBGs in SMF-SCMCF structure was examined by increasing the transverse load from 0 to 0.4 N/mm and the corresponding changes in the reflection spectrum were recorded.

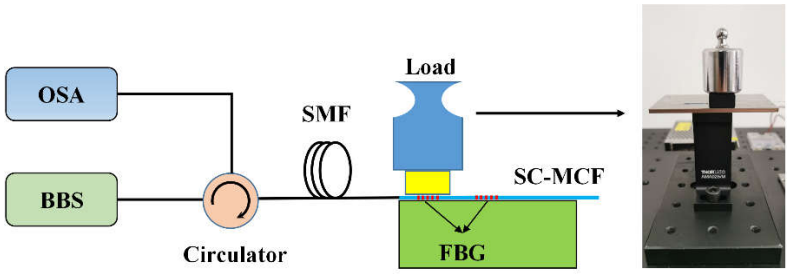

Fig.7. Schematic of the experiment setup for transverse load sensing.

The results of the aforementioned experiments are summarized in Fig. 8. It can be seen that the wavelength of the FBG in SCMCF undergoes a blue shift with increasing transverse load, which has opposite response characteristic compared with temperature sensing. The transverse load sensitivities of the two FBGs are -153.3 pm/ (N/mm) and -157.3 pm/ (N/mm), with linearity of R^2=0.993 and R^2=0.994, respectively. We ascribe the small discrepancy in sensitivity to the fact that measurement error caused by the limited spectrum resolution of the adopted OSA. It should be pointed out that the sensitivity of the proposed sensor is lower compared with the previous works based on silica microsphere [34, 35]. However, the proposed device has a more robust structure for high transverse load sensing.

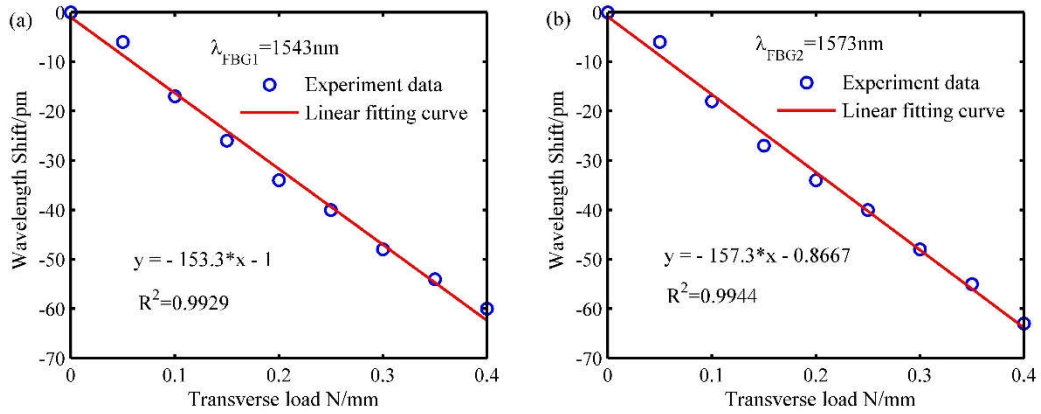

Fig.8 The wavelength shift of the two FBGs versus transverse load. (a) FBG1; (b) FBG2.

In order to investigate the sensor's repeatability and reliability, a cycling test of transverse load was conducted. The transverse load was initially set at 0 N/mm, then increased to 0.4 N/mm, with a step size of 0.05 N/mm. The test was repeated with 3 cycles, as shown in Fig.9. The maximum discrepancy is observed to be less than 2 pm and 4 pm for FBG1 and FBG2, with the corresponding transverse loading uncertainty of 0.013 N/mm and 0.025 N/mm, showing that the proposed sensor is highly reversible with very low hysteresis.

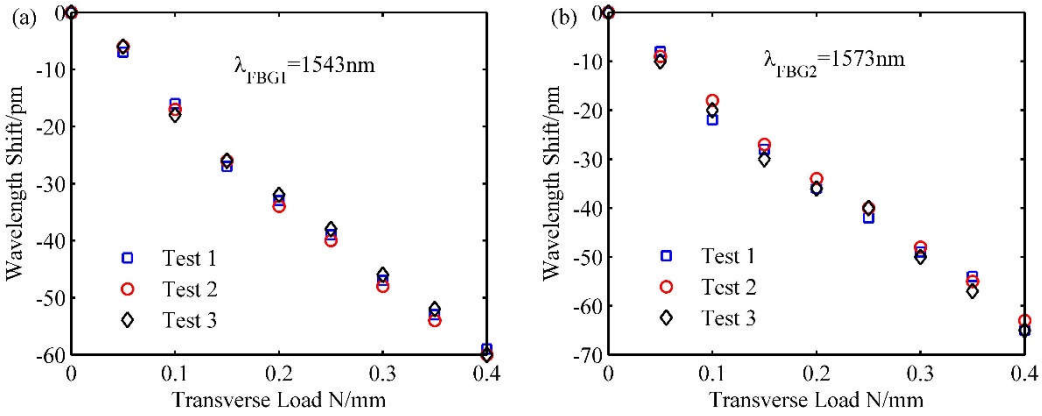

Fig.9 Repeated testing of wavelength shift versus transverse load. (a) FBG1; (b) FBG2.

The proposed SCMCF-FBG sensor can also be used as a vibration sensor. Unlike the temperature and transverse load testing discussed above, which is based on decoding the wavelength shift of FBG, periodic shifts of the reflection pattern of the SMF-SCMCF were correlated with vibration. To induce vibrations to the SMF-SCMCF structure, it was placed in cantilever position as shown in Fig. 10. Note that the clamping point is located at the SMF because the SCMCF is sensitive to local pressure. A piezo-electric transducer (PZT) directly contact with the clamping point and is driven by a function generator to shake the SMF-SCMCF structure. The periodic bending of the SCMCF induces cyclic changes of Δn, which gives rise to a periodic shift of the reflection spectrum. To monitor vibrations with our devices, a miniature spectrometer (IMON512-USB, from Ibsen Photonics, Denmark) is used. Here, the center of gravity (COG) algorithm installed in our spectrometer is adopted to track the periodic shift of the interference pattern with high speed and accuracy. On this basis, the vibration frequency is determined by applying the fast Fourier transform (FFT) algorithm to the measured wavelength shift of the interference pattern as a function of time. In a proof-of-concept experiment, the frequency of the function generator is set at 84 Hz.

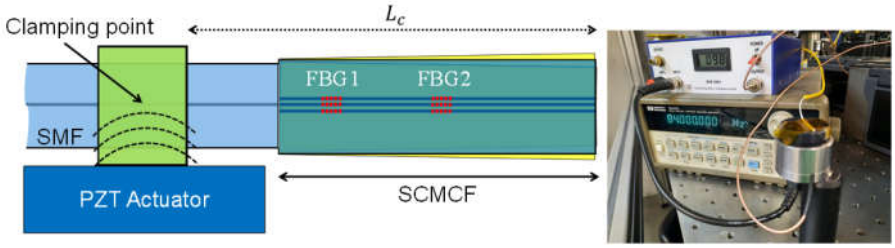

Fig. 10. Schematic of the experiment setup for vibration sensing. L_c is the length of the cantilever.

Figures 11 shows the measured vibration frequency with our proposed sensor; the inset shows the wavelength shift of the reflection pattern versus time. It can be clearly observed that the dominant peak of the FFT is located at 84 Hz, which is consistent with the applied vibration frequency. This suggests that the simple configuration shown in Fig. 10 can be used for vibrations sensing or for the development of accelerometers. It is worth noting that we do not monitor the absolute wavelength shift but the period of the shift, the issue of cross-sensitivity arises from temperature or transverse load will not affect the vibration interrogation, which enables multiparameter sensing. Furthermore, the detectable frequency range of our proposed device can be easily tailored by optimizing the length of the cantilever, as demonstrated in our previous publication [28].

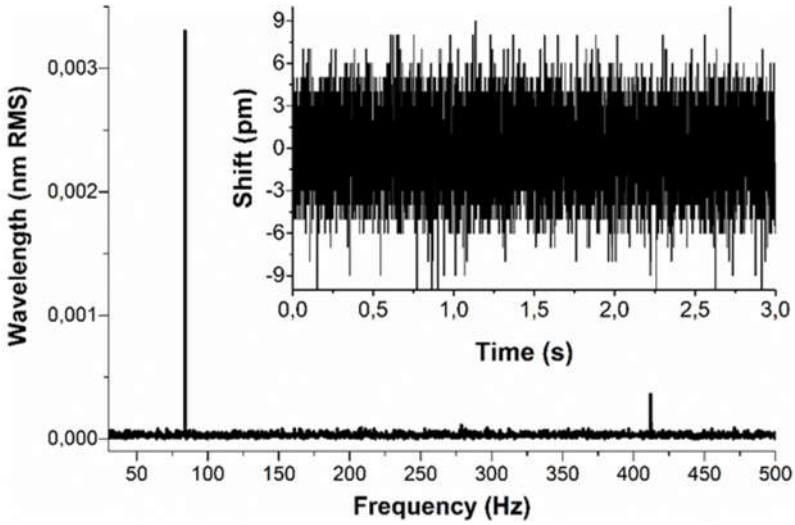

Fig. 11. The inset plots show the position of a peak of the reflection versus time when the MCF was vibrating at 84 Hz. From such a graph, the FFT was calculated. The position of the FFT peak is at 84 Hz.

Finally, we compared the performance characteristics of the proposed sensor with the other multiparameter sensors based on hybrid structure reported in the literature. Table 1 lists a few important features of these sensors for comparison. It can be observed that the proposed sensor achieves a comparable temperature sensitivity to other schemes. Although the transverse load sensitivity of the proposed sensor is lower compared with the silica-microsphere based sensors, the proposed device has better mechanical strength. Besides, most of the existing multiparameter sensors can only measure static parameters, by contrast, the proposed sensor can realize both static and dynamic sensing.

Table 1 Comparisons between the sensors for multiparameter measurement

Sensor Structure	Measurand	Sensitivity	Reference
Supermode interferometer + FBG	Temperature Transverse load Vibration	9.7 pm/°C -157.3 pm/ (N/mm)	This work
Hybrid FP interferometer	Temperature Strain	1.3 pm/°C 5.2 pm/με	[36]
FP interferometer + FBG	Temperature Strain	7.82 pm/°C 2.1 pm/με	[32]
Michelson + FP interferometer	Temperature Transverse load	12.5- 41.5 pm/°C 0.85- 1.09 nm/N	[37]
Balloon-like interferometer + FBG	Temperature Displacement	105 pm/°C 180 pm/μm	[31]

IV. CONCLUSION

In conclusion, a simple and compact multipoint and multiparameter sensor by embedding two

FBGs into the SCMCF-based device is proposed and experimentally demonstrated. The device here proposed operators in reflection mode. One end of the SCMCF with FBGs inscribed is fusion spliced to the SMF and the other end is cleaved. We demonstrated that the FBG inscribed in SCMCF has a good linear response to temperature and transverse load with the sensitivities of 9.7 pm/°C, and -157.3 pm/(N/mm), respectively. By virtue of wavelength division multiplexing, cascaded FBGs with different wavelength enable the capability of multipoint sensing along the length of the fiber. Additionally, the vibration sensing with high precision is validated by tracking the periodic shift of the reflection spectrum. The issue of cross sensitivity can be effectively eliminated by monitoring the periodic shift of the reflection spectrum instead of the absolute wavelength change, which is beneficial to realize multiparameter sensing. The main advantage of the sensor proposed here include compactness, low cost, ease of interrogation. In addition, the experimental results show that the combination of FBG and SCMCF-based structure is an effective way to realize multiparameter and multipoint sensing. It is believed that the sensing configuration proposed here can be attractive to the fiber optic sensor community as it can be adapted for the development of new functional fiber optic sensors.

Acknowledgments

Funding. This work was supported in part by National Natural Science Foundation of China (61922069, 61735015), the "111" Plan (B18045), Sichuan Science and Technology Program (2020YJ0329), and the Spanish Ministry of Economy and Competitiveness under the project DIMENSION TEC2017 88029-R. J.V. acknowledges funding from the Fondo Europeo de Desarrollo Regional (FEDER) and the Ministerio de Economia y Competitividad (Spain) under project PGC2018-101997-B-I00.

References

[1] H. Wang, P. Xiang, L. Jiang, Strain transfer theory of industrialized optical fiber-based sensors in civil engineering: A review on measurement accuracy, design and calibration, Sensor Actuat A-Phys. 285 (2019) 414-426.

[2] Y. J. Rao, In-fiber Bragg grating sensors, Meas. Sci. Technol. 8 (1997) 355-375.

[3] X. Shu, L. Zhang, I. Bennion, Sensitivity characteristics of long period fiber gratings, IEEE J. Lightwave Technol. 20(2) (2002) 255-266.

[4] S. Bandyopadhyay, L. Shao, M. Smietana, C. Wang, J. Hu, W. He, G. Gu and Y. Yang, Employing higher order cladding modes of fiber Bragg grating for analysis of refractive index change in volume and at the surface, IEEE Photon. J. 12(1) (2020) 7100313.

[5] Y. Wang, D. N. Wang, C. R. Liao, T. Hu, J. Guo, H. Wei, Temperature insensitive refractive index sensing by use of micro Fabry–Perot cavity based on simplified hollow-core photonic crystal fiber, Opt. Lett. 38(3) (2013) 269-271.

[6] S. Zhou, B. Huang, X. Shu, A multi-core fiber based interferometer for high temperature sensing, Meas. Sci. Technol. 28(4) (2017) 045107.

[7] Z. Tong, Y. Guo, X. Yang, Y. Cao, Simultaneous measurement of temperature and refractive Index using a fiber Bragg grating and a multimode fiber, Appl. Mech. Mater. 130 (2017) 4053-4056.

[8] H. Xiang, Y. Jiang, Fiber Bragg grating inscription in multi-core photonic crystal fiber by femtosecond laser, Optik. 171 (2018) 9-14.

[9] M. Zou, Y. Dai, X. Zhou, K. Dong, M. Yang, Femtosecond laser ablated FBG with composite microstructure for hydrogen sensor application sensors, IEEE Sensors J. 16 (2016) 2040.

[10] C. Broadway, R. Min, A. G. Leal-Junior, C. Marques, C. Caucheteur, Toward commercial polymer fiber Bragg grating sensors: review and applications, IEEE J. Lightwave Technol. 37(11) (2019) 2605-2615.

[11] R. Min, L. Pereira, T. Paixao, G. Woyessa, P. Andre, O. Bang, P. Antunes, J. Pinto, Z. Li, B. Ortega, C. Marques, Inscription of Bragg gratings in undoped PMMA mPOF with Nd: YAG laser at 266 nm wavelength, Opt. Express. 27(26) (2019) 38039-38048.

[12] A. G. Leal-Junior, A. Theodosiou, C. Marques, M. J. Pontes, K. Kalli, A. Frizera, Compensation method for temperature cross-sensitivity in transverse force applications with FBG sensors in POFs, IEEE J. Lightwave Technol. 36(17) (2018) 3360-3365.

[13] D. Zheng, J. Madrigal, H. Chen, D. Barrera, S. Sales, Multicore fiber Bragg grating based directional curvature sensor interrogated by broadband source with sinusoidal spectrum, Opt. Lett. 42 (18) (2017) 3710-3713.

[14] Y. Zhang, W. Zhang, Y. Zhang, S. Wang, L. Yu, Y. Yan, Simultaneous measurement of curvature and temperature based on LP11 mode Bragg grating in seven-core fiber, Meas. Sci. Technol. 28 (2017) 055101.

[15] J. Madrigal, D. Barrera, S. Sales, Refractive index and temperature sensing using inter-core crosstalk in multicore fibers, IEEE J. Lightwave Technol. 37(18) (2019) 4703-4709.

[16] J. Madrigal, D. Barrera, S. Sales, Regenerated fiber Bragg gratings in multicore fiber for multi-parameter sensing, IEEE J. Quantum Electron. 26(4) (2020).

[17] Y. Liu, A. Zhou, Q. Xia, Y. Zhao, H. Deng, S. Yang, L. Yuan, Quasi-distributed directional bending sensor based on fiber Bragg gratings array in triangle-four core fiber, IEEE Sensors J. 19(22) (2019) 10728 - 10735.

[18] H. Zhang, Z. Wu, P. Shum, R. Wang, X. Dinh, S. Fu, W. Tong, M. Tang, Fiber Bragg gratings in heterogeneous multicore fiber for directional bending sensing, J. Opt. 18 (2016) 085705.

[19] I. Floris, J. Madrigal, S. Sales a, P. A. Calderón, J. M. Adam, Twisting measurement and compensation of optical shape sensor based on spun multicore fiber, Mech. Syst. Signal Process. 140 (2020) 10670.

[20] D. Zheng, Z. Y. Cai, I. Floris, J. Madrigal, W. Pan, X. H. Zou, S. Sales, Temperature-insensitive optical tilt sensor based on a single eccentric-core fiber Bragg grating, Opt. Lett. 44(22) (2019) 5570-5573.

[21] A. Fender, W. N. MacPherson, R. R. Maier, J. S. Barton, D. S. George, R. I. Howden, G. W. Smith, B. J. S. Jones, S. McCulloch, X. F. Chen, R. Suo, L. Zhang, I. Bennion, Two-axis temperature-insensitive accelerometer based on multicore fiber Bragg gratings, IEEE Sensors J. 8(7) (2008) 1292-1298.

[22] J. P. Moore and M. D. Rogge, Shape sensing using multi-core fiber optic cable and parametric curve solutions, Opt. Express. 20(3) (2012) 2976-2973.

[23] M. J. Gander, W. N. MacPherson, R. McBride, J. D. C. Jones, L. Zhang, I. Bennion, P. M. Blanchard, J. G. Burnett, A. H. Greenaway, Bend measurement using Bragg gratings in multi-core fiber, Electron. Lett. 36(2) (2000) 120-121.

[24] G. M. H. Flockhart, W. N. MacPherson, J. S. Barton, J. D. C. Jones, L. Zhang, I. Bennion, Two-axis bend measurement with Bragg gratings in multicore optical fiber, Opt. Lett. 28(6) (2003) 387-389.

[25] D. Barrera, I. Gasulla, S. Sales, Multipoint two-dimensional curvature optical fiber sensor based on a nontwisted homogeneous four-core fiber, IEEE J. Lightwave Technol. 33(12) (2015) 2445-2450.

[26] J. Wei, S. Wang, J. Li, S. Zuo, Novel integrated helical design of single optic fiber for shape sensing of flexible robot, IEEE Sensors J. 17(20) (2017) 6627-6636.

[27] J Antonio-Lopez, Z. Eznaveh, P. LiKamWa, A. Schülzgen, R. Amezcua-Correa, Multicore fiber sensor for high-temperature applications up to 1000°C, Opt. Lett. 39(15) (2014) 4309-4312.

[28] J. Villatoro, J. Antonio-Lopez, J. Zubia, A. Schülzgen, R. Amezcua-Correa, Interferometer based on strongly coupled multi-core optical fiber for accurate vibration sensing, Opt. Express. 25(21) (2017) 25734-25740.

[29] J. Villatoro, O. Arrizabalaga, G. Durana, I. S. Ocariz, E. Antonio-Lopez, J. Zubia, A. Schülzgen, R. Amezcua-Correa, Accurate strain sensing based on super-mode interference in strongly coupled multi-core optical fibres, Sci. Rep. 7(2017) 4451.

[30] Y. Wang, Q. Huang, W. Zhu, M. Yang, Simultaneous measurement of temperature and relative humidity based on FBG and FP interferometer, IEEE Photon. Technol. Lett. 30(9) (2018) 833-836.

[31] Y. Wu, F. Meng, H. Li, G. Yan, L. Zhu, Simultaneous measurement of micro-displacement and temperature based on balloon-like interferometer and fiber Bragg grating, Optik. 183(2019) 875-880.

[32] X. Zhang, W. Peng, L. Shao, W. Pan, L. Yan, Fiber-optic hybrid structure sensor for simultaneous measurement of transverse load and temperature, Sensor Actuat A-Phys. 272 (2018) 134-138.

[33] N. Kishi and E. Yamashita, A simple coupled-mode analysis method for multiple-core optical fiber and coupled dielectric waveguide structures, IEEE Trans. Microwave Theory Tech. 36 (1988) 1861–1868.

[34] Y. F. Wu, B. Liu, J. Wu, L. L Zhao, T. T. Sun, Y. Y. Mao, T. Nan, J. Wang, A transverse load sensor with ultra-sensitivity employing Vernier-effect improved parallel-structured fiber-optic Fabry-Perot interferometer, IEEE Access. 7 (2019) 120297-120303.

[35] S. Novais, M. S. Ferreira, J. L. Pinto, Lateral load sensing with an optical fiber inline microcavity, IEEE Photon. Technol. Lett. 29 (17) (2017) 1502–1505.

[36] A. Zhou, B. Qin, Z. Zhu, Y. Zhang, Z. Liu, J. Yang, L. Yuan, Hybrid structured fiber-optic Fabry–Perot interferometer for simultaneous measurement of strain and temperature, Opt. Lett. 39(18) (2014) 5267-5269.

[37] F. Zhu, Y. Zhang, Y. Qu, H. Su. L. Zhao, Y. Guo, Fiber-optic hybrid structure sensor for simultaneous measurement of transverse load and temperature, Optik. 208 (2020) 164078.